

CIAMA: A Multiple Access Scheme with High Diversity and Multiplexing Gains for Next-gen Wireless Networks

Jianjian Wu, Chi-Tsun Cheng, *Senior Member, IEEE*, Qingfeng Zhou, *Member, IEEE*

Abstract—This paper studies advanced multi-access techniques to support high volumes of concurrent access in wireless networks. Sparse code multiple access (SCMA), as a code-domain Non-Orthogonal Multiple Access (NOMA), serves multiple users simultaneously by adopting frequency-domain coding. Blind Interference Alignment, in contrast, applies time-domain coding to accommodate multiple users. Unlike beamforming, both of them need no Channel State Information at the Transmitter (CSIT), which saves control overheads on channel information feedback. To further increase multiplexing gain and diversity order, we propose a new multiple access framework, which utilizes both time and frequency coding by combining SCMA and BIA, which is CIAMA (sparseCode-and-bIA-based multiple access). Two decoding schemes, namely the two-stage decoding scheme consisting of zero-forcing and Message Passing Algorithm (MPA), and the Joint Message Passing Algorithm (JMPA) enhanced by constructing a virtual factor graph, have been analyzed. Simulation results indicate that although the performance of the two-stage decoding scheme is inferior to both BIA and SCMA, it has a relatively low decoding complexity. Nonetheless, the JMPA decoding scheme achieves the same diversity gain as an STBC-based SCMA and with an even higher multiplexing gain, which makes the CIAMA with JMPA decoding scheme a promising MA scheme for next-gen wireless networks.

Index Terms—Multiple access, Sparse-code multiple access (SCMA), Blind interference alignment (BIA).

I. INTRODUCTION

Managing concurrent access is continuously as one of the biggest challenge in wireless networks. To meet the growing need for connectivity, fifth-generation (5G) wireless networks implement various technologies, such as massive Multiple Input Multiple Output (MIMO) and millimeter microwave (mm-Wave) [1], to alleviate the corresponding issues. The increasing deployment of micro-cells to enhance data transfer rates and densify network connections further complicates multi-user access [2], [3]. While research and industrial institutes have been developing advance technologies to migrate existing communication systems towards their sixth-generation (6G), with an approximately 100 times higher capacity than 5G, the underlying problems associated with concurrent access can be bigger than ever [4].

Corresponding author: Qingfeng Zhou (e-mail: enqfzhou@ieee.org). J.Wu and Q.F.zhou are with the School of Electric Engineering and Intelligentization, Dongguan University of Technology, Dongguan 523808, China. J.Wu and Q.F.zhou are with the Dongguan Key Lab of Artificial Information Network C.-T. Cheng is with the Department of Manufacturing, Materials and Mechatronics, RMIT University, Melbourne, VIC 3000, Australia (e-mail: ben.cheng@rmit.edu.au).

Orthogonal techniques such as Frequency Division Multiple Access (FDMA), Time Division Multiple Access (TDMA), Code Division Multiple Access (CDMA), and Orthogonal Frequency Division Multiple Access (OFDMA) have been used to manage multi-user interference in conventional wireless communication systems [5]. These techniques divide wireless resource in an orthogonal manner, enabling the exclusive access to a fraction of the wireless resource by individual user, thereby avoiding interference [6]. However, such an approach does not scale well with the increasing concurrent access demands. To attain higher spectral efficiency, researchers have been exploring non-orthogonal techniques such as Interference alignment (IA) [7] and Non-Orthogonal Multiple Access (NOMA) [8]. IA aligns multiple interference signal vectors into a small subspace and reserves the remaining subspace for transmitting the intended signal [9]. Given its potential to reach the capacity of interference channels, researchers have incorporated IA into several communication systems [10], including cognitive radio networks [11], cellular networks [12], heterogeneous networks [13], and Device-to-Device (D2D) networks [14]. NOMA utilizes superposition coding to allow multiple users to transmit signals on the same resource block, for instance, time and frequency. There are two major types of NOMA, namely Power-Domain NOMA (PD-NOMA) and Code-Domain NOMA (CD-NOMA) [15]. Signals at the receivers are decoded using Successive Interference Cancellation (SIC) or Message Passing Algorithm (MPA). NOMA can combine with other existing technologies such as massive MIMO [16], mm-Wave [17], etc.. NOMA has been being one of the focuses in the research on 5G communications and is expected to be a key research area in future generations of wireless networks.

Throughout the development of IA, a primary limitation is the requirement for channel state information at the transmitter (CSIT) [18]. In order to eliminate the dependency on CSIT, blind IA (BIA) was introduced in [19]. BIA works under predefined channel patterns and can be fulfilled by two methods: channel-based BIA (CB-BIA) [20] and reconfigurable-antenna-based BIA (RA-BIA). BIA carries out transmissions using specially designed channel patterns, often referred to as "supersymbols," over several symbol extensions. The overhead cost associated with mode-switching in RA-BIA is has been studied in [21], and methods have been proposed to achieve the minimum overall number of mode-switching instances among various users. Furthermore, a balanced-switching-oriented BIA plan has been formulated, which maintains a similar total

number of mode-switching instances as those of the schemes under the same study [22]. Moreover, Menon and Selvaprabhu provide a comprehensive survey on BIA in [23].

PD-NOMA schemes also require information on channel information [24]. With CSIT available, IA has been introduced into PD-NOMA systems in [25]. Hybrid schemes are typically more practical compared to IA-only schemes and exhibit superior performance relative to NOMA-only systems. For instance, IA is employed to manage inter-cell and inter-cluster interferences in multi-cell NOMA systems [26]. In light of the additional overhead involved with CSIT, Morales-Céspedes *et al.* have introduced blind IA (BIA) into PD-NOMA systems, as discussed in [27]. According to their suggested scheme, BIA effectively mitigates interferences between clusters without the need for moment-by-moment access to CSIT, and offers better results compared to conventional MISO-NOMA techniques. While the proposed scheme is independent of instantaneous CSIT, its integration into multi-carrier systems is not straightforward [27].

PD-NOMA techniques typically require CSIT for efficient power allocation, which limits their applicability in systems with limited or no access to CSIT. To fit such systems, the sparse code multiple access (SCMA) technique is more feasible alternative in code-domain NOMA, as highlighted in [28]. In multi-carrier systems, both low-density multi-dimensional codebooks and message passing algorithms (MPA) are employed, which provide multi-subcarrier diversity gain and unique "shaping gain" to facilitate SCMA, as explained in [29]. The optimal codebook design for SCMA has not yet been found due to its complexity. Chen *et al.* in [30] suggest a low-complexity construction method as well as a systematic construction process for the near-optimal codebook design. The low-complexity decoding architecture of SCMA is also a hot topic. Scholars have attempted to simplify the task by adapting MPA to the logarithmic domain, proposing techniques such as Log-MPA and MAX-Log-MPA, which reduce the number of exponential operations required in the original MPA. While low-complexity MPA techniques have been proposed, the design of decoders for MIMO-SCMA systems remains challenging because the decoding complexity increases exponentially with the number of users [31]. Additionally, Pan *et al.* have incorporated space-time block coding (STBC) into MIMO-SCMA systems, which offers a higher diversity order [32]. Although the STBC-SCMA scheme offers additional diversity over multiple antennas, its multiplexing gain is limited. Another limitation of existing SCMA schemes is the potential for privacy breaches in multi-user systems. In such systems, each receiver uses MPA to decode not only the desired signal, but also interference signals, as multi-user signals are simply superimposed over the code domain, which can allow for unauthorized access to data from other users.

BIA and SCMA have the potential to adapt to systems with partial or no channel state information, making these two techniques more robust than other CSIT-based methods. BIA and SCMA are implemented in different domains, and they use different interference management principles. Specifically BIA eliminates interference before decoding, while SCMA treats interference as noise when decoding. So the combination

of BIA and SCMA is non-trivial and cannot be achieved by concatenating them. This paper aims to fill such a research gap, and proposes an effective method to combine SCMA and BIA while achieving even higher diversity order and multiplexing gain. In our proposed scheme, transmitted signals are first mapped by SCMA codebooks, and the resulting codewords are then encoded using the BIA principle. At the receiver, two decoding schemes are employed. The first is a two-stage scheme that employs zero-forcing and then a MPA. The second scheme is the joint MPA (JMPA), and the key to the implementation is to construct a virtual factor graph. The complexity of the two-stage decoder grows linearly with the number of users, but its performance is limited. The JMPA decoder achieves the same diversity order as the space-time block coded SCMA (STBC-SCMA) scheme, with the same cost of complexity. Our proposed scheme is suitable for systems lacking instantaneous channel state information and achieves a higher multiplexing gain while maintaining the same diversity gain as STBC-SCMA. Moreover, our scheme performs better on data privacy existing MIMO-SCMA schemes, since we employ BIA to manage multi-user interference.

The rest of this paper is organized as follows. Section.II briefly describes the system model and introduces the principle of BIA and SCMA. In section.III, a SparseCode-and-BIA-based multiple access (CIAMA) scheme is proposed, including both the encoding design and two decoding designs. In Section IV, we derive a closed-form expression for the average pairwise error probability (PEP) of CIAMA, which provides a universal bound for bit error rate (BER). Section.V illustrates the simulation results, and finally section.VI concludes this paper.

II. SYSTEM MODEL

Consider a K -user $N_t \times 1$ MISO broadcast channel with J tones, e.g., OFDM subcarriers, available for transmission. To ease understanding, in the following derivations, it is assumed that $K = 6$, $J = 4$, the base station has $N_t = 2$ traditional antennas, and each receiver/user equips a reconfigurable antenna (RA). The same assumption has been adopted in previous studies on RA-based BIA. Here, we suppose a RA can artificially switch its operation mode, thus change its channel state. The RA can switch $N_t = 2$ modes at each user. In this paper, we suppose no CSI at the BS but full CSI at all receivers.

The composite channel model applied considers both quasi-static Rayleigh fading and large-scale path loss. Denote $\mathbf{h}_k^j(m) = \frac{\mathbf{g}_k^j(m)}{\sqrt{D(d_k)}}$ as the channel matrix from the base station to the Rx- k while its RA operating at the m -th mode on the j -th tones, where $\mathbf{h}_k^j, \mathbf{g}_k^j(m) \in \mathbb{C}^{1 \times N_t}$ and $\mathbf{g}_k^j(m)$ denotes a Rayleigh fading channel matrix. d_k is the distance between the k -th user and the BS. The path loss function is denoted as

$$D(d_k) = \begin{cases} d_k^\alpha, & \text{if } d_k > r_0 \\ r_0^\alpha, & \text{otherwise} \end{cases},$$

where α denotes the path loss exponent and the parameter r_0 avoids a singularity when the distance is small. Without

TABLE I
SUPERSYMBOL OF BIA

	slot-1	slot-2	slot-3	slot-4	slot-5	slot-6	slot-7
R_1	$\mathbf{h}_1^j(1)$	$\mathbf{h}_1^j(2)$	$\mathbf{h}_1^j(1)$	$\mathbf{h}_1^j(1)$	$\mathbf{h}_1^j(1)$	$\mathbf{h}_1^j(1)$	$\mathbf{h}_1^j(1)$
R_2	$\mathbf{h}_2^j(1)$	$\mathbf{h}_2^j(1)$	$\mathbf{h}_2^j(2)$	$\mathbf{h}_2^j(1)$	$\mathbf{h}_2^j(1)$	$\mathbf{h}_2^j(1)$	$\mathbf{h}_2^j(1)$
R_3	$\mathbf{h}_3^j(1)$	$\mathbf{h}_3^j(1)$	$\mathbf{h}_3^j(1)$	$\mathbf{h}_3^j(2)$	$\mathbf{h}_3^j(1)$	$\mathbf{h}_3^j(1)$	$\mathbf{h}_3^j(1)$
R_4	$\mathbf{h}_4^j(1)$	$\mathbf{h}_4^j(1)$	$\mathbf{h}_4^j(1)$	$\mathbf{h}_4^j(1)$	$\mathbf{h}_4^j(2)$	$\mathbf{h}_4^j(1)$	$\mathbf{h}_4^j(1)$
R_5	$\mathbf{h}_5^j(1)$	$\mathbf{h}_5^j(1)$	$\mathbf{h}_5^j(1)$	$\mathbf{h}_5^j(1)$	$\mathbf{h}_5^j(1)$	$\mathbf{h}_5^j(2)$	$\mathbf{h}_5^j(1)$
R_6	$\mathbf{h}_6^j(1)$	$\mathbf{h}_6^j(1)$	$\mathbf{h}_6^j(1)$	$\mathbf{h}_6^j(1)$	$\mathbf{h}_6^j(1)$	$\mathbf{h}_6^j(1)$	$\mathbf{h}_6^j(2)$

R_1	$\mathbf{V}_1 = [\mathbf{I} \mathbf{1} \mathbf{0} \mathbf{0} \mathbf{0} \mathbf{0} \mathbf{0}]^T$
R_2	$\mathbf{V}_2 = [\mathbf{1} \mathbf{0} \mathbf{1} \mathbf{0} \mathbf{0} \mathbf{0} \mathbf{0}]^T$
R_3	$\mathbf{V}_3 = [\mathbf{1} \mathbf{0} \mathbf{0} \mathbf{1} \mathbf{0} \mathbf{0} \mathbf{0}]^T$
R_4	$\mathbf{V}_4 = [\mathbf{1} \mathbf{0} \mathbf{0} \mathbf{0} \mathbf{1} \mathbf{0} \mathbf{0}]^T$
R_5	$\mathbf{V}_5 = [\mathbf{1} \mathbf{0} \mathbf{0} \mathbf{0} \mathbf{0} \mathbf{1} \mathbf{0}]^T$
R_6	$\mathbf{V}_6 = [\mathbf{1} \mathbf{1} \mathbf{0} \mathbf{0} \mathbf{0} \mathbf{0} \mathbf{1}]^T$

Fig. 1. Beamforming vectors of BIA

loss of generality, we choose $\alpha = 3$. Note that we assume the channel state over different antennas and tones are independent and the coherence time over all channels is long enough, e.g., each channel state keeps unchanged over a whole transmission progress. We further denotes E_s as the total transmit power at the BS.

A. Blind Interference alignment

In this section, the BIA scheme based on RA is utilized in the system [19]. It is assumed that RA can switch their operation mode and hence artificially change the channel state. By leveraging this property, we utilize RA to artificially reconstruct the channel patterns, hence satisfying feasible conditions for BIA. The result channel patterns are denoted as ‘‘supersymbols’’. To decode intended signals, a decoding beamforming vector is designed for each user, respectively. As an example, the supersymbol and transmit beamforming vectors \mathbf{V}_k on the j -th tone can be shown as Table.I and Fig. 1, respectively. Note that $\mathbf{0}$ denotes a all-zero matrix with the size of 2×2 . Here we consider independent BIA design at each subcarrier.

Without loss of generality, Consider the j -th tones at the

first user , the received signal can be expressed as

$$\begin{aligned} \mathbf{Y}_1^j &= \mathcal{H}_1^j \left(\mathbf{V}_1 \mathbf{u}_1^j + \mathbf{V}_2 \mathbf{u}_2^j + \mathbf{V}_3 \mathbf{u}_3^j + \mathbf{V}_4 \mathbf{u}_4^j + \mathbf{V}_5 \mathbf{u}_5^j + \mathbf{V}_6 \mathbf{u}_6^j \right) + \mathbf{Z}_1^j \\ &= \begin{bmatrix} \mathbf{h}_1^j(1) \\ \mathbf{h}_1^j(2) \\ \mathbf{0} \\ \mathbf{0} \\ \mathbf{0} \\ \mathbf{0} \end{bmatrix} \mathbf{u}_1^j + \begin{bmatrix} \mathbf{h}_1^j(1) \\ \mathbf{0} \\ \mathbf{h}_1^j(1) \\ \mathbf{0} \\ \mathbf{0} \\ \mathbf{0} \end{bmatrix} \mathbf{u}_2^j + \begin{bmatrix} \mathbf{h}_1^j(1) \\ \mathbf{0} \\ \mathbf{0} \\ \mathbf{h}_1^j(1) \\ \mathbf{0} \\ \mathbf{0} \end{bmatrix} \mathbf{u}_3^j \\ &+ \begin{bmatrix} \mathbf{h}_1^j(1) \\ \mathbf{0} \\ \mathbf{0} \\ \mathbf{h}_1^j(1) \\ \mathbf{0} \\ \mathbf{0} \end{bmatrix} \mathbf{u}_4^j + \begin{bmatrix} \mathbf{h}_1^j(1) \\ \mathbf{0} \\ \mathbf{0} \\ \mathbf{0} \\ \mathbf{h}_1^j(1) \\ \mathbf{0} \end{bmatrix} \mathbf{u}_5^j + \begin{bmatrix} \mathbf{h}_1^j(1) \\ \mathbf{0} \\ \mathbf{0} \\ \mathbf{0} \\ \mathbf{0} \\ \mathbf{h}_1^j(1) \end{bmatrix} \mathbf{u}_6^j \\ &+ \mathbf{Z}_1^j \end{aligned} \quad (1)$$

where

$$\mathcal{H}_1^j = \begin{bmatrix} \mathbf{h}_1^j(1) & \mathbf{0} & \dots & \dots & \dots & \dots & \mathbf{0} \\ \mathbf{0} & \mathbf{h}_1^j(2) & & & & & \vdots \\ \vdots & & \mathbf{h}_1^j(1) & & & & \vdots \\ \vdots & & & \mathbf{h}_1^j(1) & & & \vdots \\ \vdots & & & & \mathbf{h}_1^j(1) & & \vdots \\ \vdots & & & & & \mathbf{h}_1^j(1) & \mathbf{0} \\ \mathbf{0} & \dots & \dots & \dots & \mathbf{0} & \dots & \mathbf{h}_1^j(1) \end{bmatrix} \quad (2)$$

is the corresponding channel matrix according to the supersymbol and $\mathbf{u}_k^j \in \mathbb{C}^{N_t \times 1}$ is the transmit complex vector for the k -th user at the j -th tone. For decoding its desired signals, a post-processing matrix

$$\mathbf{P}_1 = \begin{bmatrix} \frac{1}{\sqrt{6}} & 0 & -\frac{1}{\sqrt{6}} & -\frac{1}{\sqrt{6}} & -\frac{1}{\sqrt{6}} & -\frac{1}{\sqrt{6}} & -\frac{1}{\sqrt{6}} \\ 0 & 1 & 0 & 0 & 0 & 0 & 0 \end{bmatrix} \quad (3)$$

is utilized, hence we have

$$\mathbf{P}_1 \mathbf{Y}_1^j = \begin{bmatrix} \frac{1}{\sqrt{6}} \mathbf{h}_1^j(1) \\ \mathbf{h}_1^j(2) \end{bmatrix} \mathbf{u}_1^j + \tilde{\mathbf{Z}}_1^j. \quad (4)$$

Consequently an equivalent 2×2 MIMO channel is achieved and traditional MIMO detectors can be readily introduced, e.g., zero-forcing decoder and MMSE decoder.

B. Sparse code multiple access

In this section, traditional SCMA scheme is introduced. Fig. 2 shows the multi-antenna SCMA transceiver diagram, which is composed of the encoding process and the k -th user’s decoder design. Note that the joint MPA (JMPA) is used to decode all transmitting signals.

In this model, $b_k^{(n_t)}$ denotes the binary input for the k -th user at the n_t -th antenna. After the SCMA encoder, $b_k^{(n_t)}$ is mapped to a complex codeword $\mathbf{s}_k^{(n_t)} = [s_k^{1(n_t)}, \dots, s_k^{J(n_t)}]^T$ for user- k from the n_t -th antenna over J subcarriers. Denotes

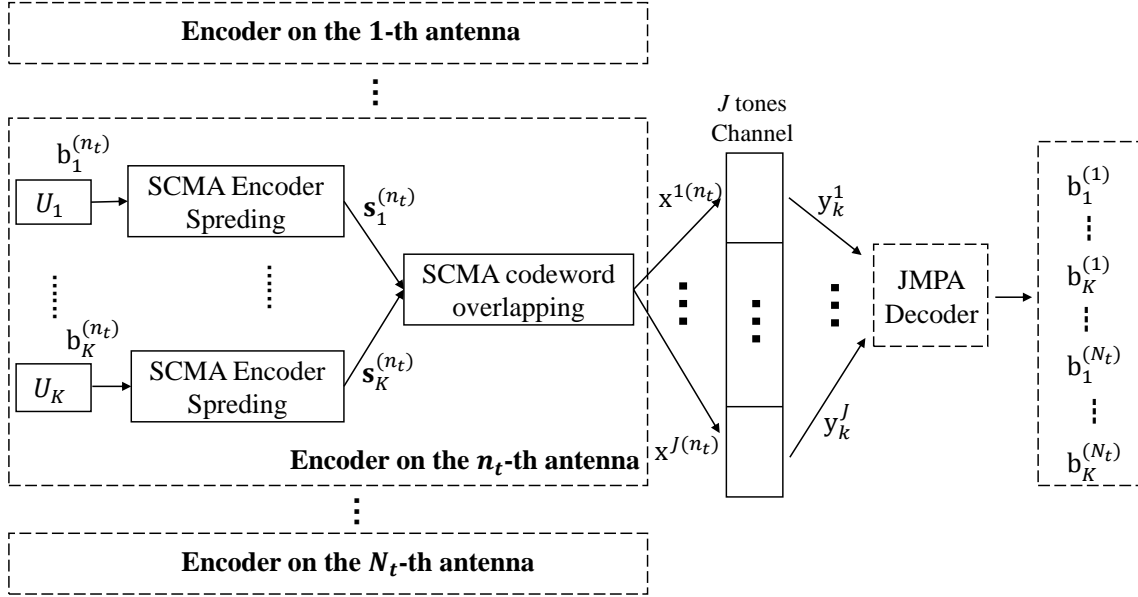


Fig. 2. Transceiver diagram of Multi-antenna SCMA.

an indicator matrix as $F = [f_1 \ \cdots \ f_K]$, where '1' in f_k denotes the positions of non-zero elements in $\mathbf{s}_k^{(n_t)}$. What the assumptions that $K = 6$ and $J = 4$, the indicator matrix is then denoted as

$$F = \begin{bmatrix} 1 & 1 & 1 & 0 & 0 & 0 \\ 1 & 0 & 0 & 1 & 1 & 0 \\ 0 & 1 & 0 & 1 & 0 & 1 \\ 0 & 0 & 1 & 0 & 1 & 1 \end{bmatrix}. \quad (5)$$

Note that the indicator matrix design influence the decoding complexity and accuracy, the one adopted above is designed to yield a moderate performance and computation consumption. Here, all user are using different sets of tones.

The received signal of user- k is written as

$$\mathbf{y}_k = \sum_{n_t=1}^{N_t} \text{diag}(\mathbf{h}_k^{(n_t)}) \mathbf{x}^{(n_t)} = \sum_{n_t=1}^{N_t} \text{diag}(\mathbf{h}_k^{(n_t)}) \sum_{i=1}^K \mathbf{s}_i^{(n_t)} + \mathbf{n}_k, \quad (6)$$

where $\mathbf{x}^{(n_t)} = [x^{1(n_t)}, \dots, x^{J(n_t)}]^T = \sum_{k=1}^K \mathbf{s}_k^{(n_t)}$ denotes the superposed signals for six users over four tones, and $\mathbf{h}_k^{(n_t)} \in \mathbb{C}^{J \times 1}$ denotes the channel coefficient vector of the n_t -th antenna of the user- k over all subcarriers.

The multi-antenna SCMA does not utilize any multi antenna gain, e.g, diversity gain and multiplexing gain. Traditional MIMO technique and space-time block code have therefore been introduced into the multi antenna SCMA system in the literature [32]. Table.II shows the conventional STBC, Alamouti code, in a two user 2×1 BC at the j -th tone. Note that in this paper we use x^* to denotes the conjugate of a complex number x . By utilizing the Alamouti code, two different symbols are transmitted over two antennas through two slots, and diversity gain is realized.

Differ from the abovementioned Multi-antenna SCMA, the STBC-SCMA employs an STBC encoder for transmitting signals from multi-antennas, thus transmitting different symbols on two antennas, i.e., $s_i^{(1)} \neq s_i^{(2)}$ and $x^{j(1)} \neq x^{j(2)}$. Therefore,

TABLE II
ALAMOUTI CODE

	slot 1	slot 2
Antenna A	$x^{j(1)}$	$-x^{j(2)*}$
Antenna B	$x^{j(2)}$	$x^{j(1)*}$

for the j -th subcarrier, $x^{j(1)}$ and $x^{j(2)}$ are transmitted through the Alamouti code over two slots.

According the Alamouti design, the received signals of the k -th user at the j -th subcarrier are

$$\begin{bmatrix} y_k^j(1) \\ y_k^{j*}(2) \end{bmatrix} = \begin{bmatrix} h_k^{j(1)} & h_k^{j(2)} \\ h_k^{j(2)*} & -h_k^{j(1)*} \end{bmatrix} \begin{bmatrix} x^{j(1)} \\ x^{j(2)} \end{bmatrix} + \begin{bmatrix} z_k^{j(1)} \\ z_k^{j(2)*} \end{bmatrix}, \quad (7)$$

$$= \begin{bmatrix} h_k^{j(1)} & h_k^{j(2)} \\ h_k^{j(2)*} & -h_k^{j(1)*} \end{bmatrix} \begin{bmatrix} \sum_{i=1}^6 s_i^{j(1)} \\ \sum_{i=1}^6 s_i^{j(2)} \end{bmatrix} + \begin{bmatrix} z_k^{j(1)} \\ z_k^{j(2)*} \end{bmatrix},$$

where $h_k^{j(n_t)}$ denotes the CSI from the n_t -th antenna of the BS to the k -th user at the j -th subcarrier.

Note that for STBC-SCMA decoder, there are two optional principles: two-stage decoder and joint MPA. The two-stage decoder is to perform a traditional linear STBC decoder, hence performing MPA. The joint MPA is to construct a virtual factor graph and performs MPA decoding according to received signals directly. Since that the decoder designs for our proposed scheme are similar to STBC-SCMA decoder, we elaborate the details of the decoder in the next section.

III. SPARSECODE-AND-BIA-BASED MA

A. Encoding design

Fig. 3 shows the transceiver diagram of the proposed design when $K = 6$, $J = 4$, and $N_t = 2$, which is composed of the encoding process and the k -th user's decoder design.

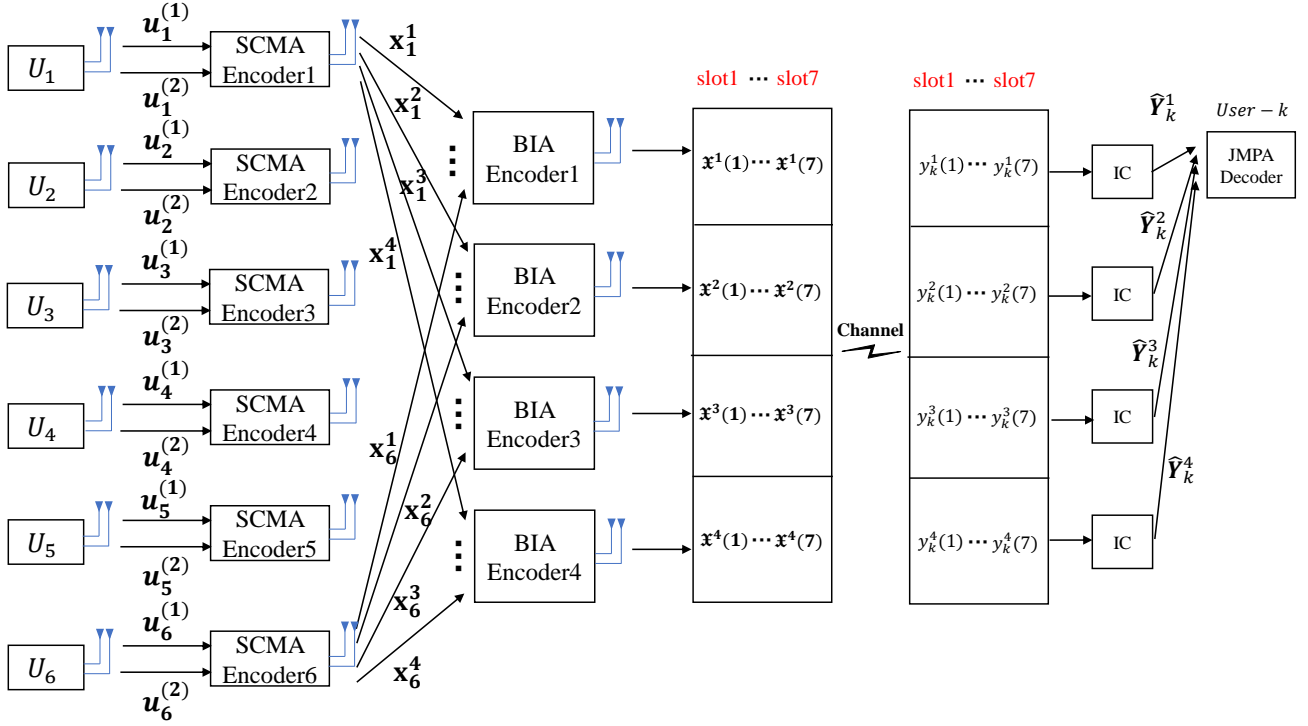


Fig. 3. Transceiver diagram of the proposed scheme

The encoding process can be presented as two steps: SCMA encoding and BIA encoding.

1) *Step 1 - SCMA encoding*: For each U_k , assume a transmitting binary vector $\mathbf{u}_k^{(n_r)}$ at the n_r -th transmit antenna, where $\mathbf{u}_k^{(n_r)}$ is a L -dimension vector. The value of L depends on the number of available subcarriers, J , and the predetermined degree of resource reuse. Here, we assume $L = 6$. For simplicity, we assume a one-bit binary variable of $u_k^{(n_r)}(i)$, i.e., the i -th element of $\mathbf{u}_k^{(n_r)}$. Note that arbitrary bits can be used, but the corresponding codebook design would be more complicated. Like traditional MIMO-SCMA systems, transmitting data $\mathbf{u}_k^{(n_r)}$ can be allocated to multiple users. For simplicity, in this paper we assume all $\mathbf{u}_k^{(n_r)}$ of U_k in Fig. 3 are for a single user.

The SCMA encoders can be defined as a mapping function $\mathfrak{f} : \mathbb{B} \rightarrow \mathcal{S}$, where $\mathcal{S} \subset \mathbb{C}^J$ and $\|\mathcal{S}\| = 2$. Thus, we have $\mathbf{s}_{ki}^{(n_r)} = \mathfrak{f}(u_k^{(n_r)}(i))$, where the SCMA codeword $\mathbf{s}_{ki}^{(n_r)} \in \mathcal{S}$ is a sparse vector and selected from $\mathcal{C}_{ki}^{(n_r)}$, i.e., the codebook of $u_k^{(n_r)}(i)$. In SCMA, the different $\mathcal{C}_{ki}^{(n_r)}$ are used for the different i . However, we can use the same codebook $\mathcal{C}_{ki}^{(n_r)}$ for different k and n_r . The reasons are: 1) Since user interference is fully eliminated by BIA, different users can share codebooks to simplify the system design. 2) The channel uncorrelation assumption allows data streams for different antennas share the same codebook. Thus, for the sake of simplicity, we use \mathcal{C}_i to denote the codebook of $u_k^{(n_r)}(i)$ for different k and n_r in the rest of the paper.

After the SCMA encoding, each element in $u_k^{(n_r)}(i)$ is mapped into a codeword and superposed over J tones, producing the transmitting symbol vector $\mathbf{S}_k^{(n_r)} = \sum_{i=1}^L \mathbf{s}_{ki}^{(n_r)} =$

$\left[\mathbf{S}_k^{1(n_r)} \dots \mathbf{S}_k^{J(n_r)} \right]^T$. Since $N_t = 2$, thus $\mathbf{S}_k^{(1)}$ and $\mathbf{S}_k^{(2)}$ are reconstructed, and for each tone we have a reconstructed symbol vector $\mathbf{x}_k^j = \left[\mathbf{S}_k^{j(1)} \mathbf{S}_k^{j(2)} \right]^T$.

2) *Step 2 - BIA encoding*: BIA encoding is applied at each tone by employing symbol extension in time domain. In this section we use the same supersymbol and beamforming vectors of BIA as shown in section.II-A. Focusing at the j -th tone, the transmit vector after reconfigurable-antenna-based BIA can be derived as

$$\mathbf{x}^j = \begin{bmatrix} \mathbf{x}^j(1) \\ \mathbf{x}^j(2) \\ \mathbf{x}^j(3) \\ \mathbf{x}^j(4) \\ \mathbf{x}^j(5) \\ \mathbf{x}^j(6) \\ \mathbf{x}^j(7) \end{bmatrix} = \begin{bmatrix} \mathbf{x}_1^j + \mathbf{x}_2^j + \mathbf{x}_3^j + \mathbf{x}_4^j + \mathbf{x}_5^j + \mathbf{x}_6^j \\ \mathbf{x}_1^j \\ \mathbf{x}_2^j \\ \mathbf{x}_3^j \\ \mathbf{x}_4^j \\ \mathbf{x}_5^j \\ \mathbf{x}_6^j \end{bmatrix} \quad (8)$$

where $\mathbf{x}_k(t) \in \mathbb{C}^{N_t \times 1}$ denotes the transmit vector from the BS in the k -th tone at the t -th slot.

After the encoding, the receive signals at the first user can be formulated as

$$\mathbf{Y}_1 = \left[(\mathbf{y}_1^1)^T \dots (\mathbf{y}_1^J)^T \right]^T \quad (9)$$

where the receive signals at on the j -th tone over 7 slots are

$$\begin{aligned} \mathbf{y}_1^j &= [y_1^j(1) \quad y_1^j(2) \quad \cdots \quad y_1^j(7)]^T \\ &= \begin{bmatrix} \mathbf{h}_1^j(1) & \mathbf{0} & \cdots & \mathbf{0} \\ \mathbf{0} & \mathbf{h}_1^j(2) & \cdots & \mathbf{0} \\ \vdots & \vdots & \ddots & \mathbf{0} \\ \mathbf{0} & \mathbf{0} & \mathbf{0} & \mathbf{h}_1^j(7) \end{bmatrix} \begin{bmatrix} \mathbf{x}^j(1) \\ \vdots \\ \mathbf{x}^j(7) \end{bmatrix} + \mathbf{Z}_1^j \end{aligned} \quad (10)$$

Here $\mathbf{Z}_1^j = [z_1^j(1) \quad \cdots \quad z_1^j(7)]^T$ is the additive gaussian noise vector over 7 slots.

B. Two stage Decoding

In this section, the proposed two-step decoding design is explained. We firstly employ a traditional MIMO detector (Zero-forcing detector) to separate space data flow, then a traditional log-MPA is applied to decode SCMA signals. By this design, low decoding complexity is achieved but the performance needs to be improved.

Based on the received signal vector, we design our decoding process by firstly applying the BIA decoder and then the MPA decoder. After the BIA decoder, multi-user interference are fully suppressed and the multiple spatial data flow can be untied. Further, each user can apply simple MPA decoder for its own data at each spatial data flow.

1) *BIA decoding*: In this step, we apply the BIA decoding for signals over each tones, respectively. The BIA decoding is composed of multi-user interference cancellation (IC) and signal detection. A multi-user IC matrix \mathbf{P}_k is firstly used for the k -th user at each tone, e.g.,

$$\mathbf{P}_1 = \begin{bmatrix} \frac{1}{\sqrt{6}} & 0 & -\frac{1}{\sqrt{6}} & -\frac{1}{\sqrt{6}} & -\frac{1}{\sqrt{6}} & -\frac{1}{\sqrt{6}} & -\frac{1}{\sqrt{6}} \\ 0 & 1 & 0 & 0 & 0 & 0 & 0 \end{bmatrix}. \quad (11)$$

Denote $\hat{\mathbf{Y}}_k^j$ as the received signal vector after the multi-user IC at the j -th tone, hence the received signals over four tones can be formulated as

$$\begin{aligned} \hat{\mathbf{Y}}_k &= \left[\left(\hat{\mathbf{Y}}_k^1 \right)^T \quad \left(\hat{\mathbf{Y}}_k^2 \right)^T \quad \left(\hat{\mathbf{Y}}_k^3 \right)^T \quad \left(\hat{\mathbf{Y}}_k^4 \right)^T \right]^T \\ &= (\mathbf{I}_4 \otimes \mathbf{P}_k) \mathbf{Y}_k \\ &= \begin{bmatrix} \mathbf{H}_k^1 & \mathbf{0} & \mathbf{0} & \mathbf{0} \\ \mathbf{0} & \mathbf{H}_k^2 & \mathbf{0} & \mathbf{0} \\ \mathbf{0} & \mathbf{0} & \mathbf{H}_k^3 & \mathbf{0} \\ \mathbf{0} & \mathbf{0} & \mathbf{0} & \mathbf{H}_k^4 \end{bmatrix} \begin{bmatrix} \mathbf{x}_k^1 \\ \mathbf{x}_k^2 \\ \mathbf{x}_k^3 \\ \mathbf{x}_k^4 \end{bmatrix} + \begin{bmatrix} \hat{\mathbf{Z}}_k^1 \\ \hat{\mathbf{Z}}_k^2 \\ \hat{\mathbf{Z}}_k^3 \\ \hat{\mathbf{Z}}_k^4 \end{bmatrix}, \quad (12) \\ &= \hat{\mathbf{H}}_k \mathbf{X}_k + \hat{\mathbf{Z}}_k \end{aligned}$$

where \otimes denotes the kronecker product and $\mathbf{H}_k^j = \left[\frac{1}{\sqrt{6}} \mathbf{h}_k^j(1) \quad \mathbf{h}_k^j(2) \right]^T \in \mathbb{C}^{2 \times 2}$ is the corresponding channel matrix for the k -th user at the j -th tone. Besides, the corresponding noise vector is

$$\hat{\mathbf{Z}}_k^j = \left[\frac{1}{\sqrt{6}} z_k^j(1) - \frac{1}{\sqrt{6}} \left(\sum_{t=3}^7 z_k^j(t) \right) \right]. \quad (13)$$

Since \mathbf{H}_k^j is full-rank, here we can simply decode each symbol of $\hat{\mathbf{Y}}_k^j$ by zero-forcing. Thus, we have untied the two spatial data flow and obtain the estimated vector $\hat{\mathbf{x}}_k^j = [\hat{x}_k^j(1) \quad \hat{x}_k^j(2)]^T$.

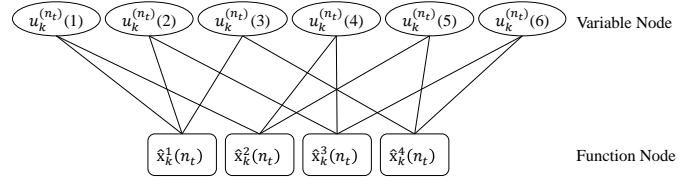


Fig. 4. Factor graph for the k -th user of the n_t -th spatial data flow when $J = 4$ and $L = 6$.

2) *MPA decoding*: Since the BIA decoder have untied the two data flows, we can apply traditional MPA decoder at each spatial data flow. Fig. 4 shows the MPA factor graph for the user-1 at one spatial data flow. Note that the MPA here has smaller computation complexity than that in SCMA, because CSI is not required in our scheme. In this step, we use $\hat{x}_k^1(n_t), \hat{x}_k^2(n_t), \hat{x}_k^3(n_t), \hat{x}_k^4(n_t)$ as function nodes, then we can decode $u_k^{(n_t)}$ at the n_t -th space data flow.

C. Joint MPA decoding

In this section, a joint MPA design is proposed, which is shown in Fig. 3. In the previous section, the ZF+MPA decoding has a poor performance considering BER because the traditional MIMO detector misfits the SCMA decoding. To further improve the performance, we propose a joint MPA design for the proposed scheme, which comes from the traditional joint MPA (JMPA) for MIMO-SCMA. As shown in Fig. 3, the proposed decoder is composed of multi-user interference cancellation (IC) blocks and a JMPA decoder.

Differ from the two stage decoding, the received signal for user- k after multi-user IC, i.e., $\hat{\mathbf{Y}}_k^j = [\hat{y}_k^j(1) \quad \cdots \quad \hat{y}_k^j(N_t)]^T$, are treated as function nodes directly then decode all space data flows simultaneously. Fig. 5 shows the virtual factor graph for the first user. The virtual indicator matrix is

$$\mathbf{F}_v = \begin{bmatrix} \mathbf{F} & \mathbf{F} \\ \mathbf{F} & \mathbf{F} \end{bmatrix}. \quad (14)$$

Further, the virtual codebook should be constructed according to the original codebook and CSI. Denotes \mathbf{C}_i as the origin codebook for $u_k^{(n_t)}(i)$. To construct the virtual codebook for the k' -th VN, we need the corresponding CSI vector $\hat{\mathbf{h}}_{k'} \in \mathbb{C}^{(N_t \times J) \times M}$. Here we define

$$\begin{bmatrix} \mathbf{A} & \mathbf{B} \\ \mathbf{C} & \mathbf{D} \end{bmatrix} = \begin{bmatrix} 1 & 0 & 0 & 0 & 0 & 0 & 0 & 0 \\ 0 & 0 & 1 & 0 & 0 & 0 & 0 & 0 \\ 0 & 0 & 0 & 0 & 1 & 0 & 0 & 0 \\ 0 & 0 & 0 & 0 & 0 & 0 & 1 & 0 \\ 0 & 1 & 0 & 0 & 0 & 0 & 0 & 0 \\ 0 & 0 & 0 & 1 & 0 & 0 & 0 & 0 \\ 0 & 0 & 0 & 0 & 0 & 1 & 0 & 0 \\ 0 & 0 & 0 & 0 & 0 & 0 & 0 & 1 \end{bmatrix} \begin{bmatrix} \mathbf{H}_1^1 \\ \mathbf{H}_1^2 \\ \mathbf{H}_1^3 \\ \mathbf{H}_1^4 \end{bmatrix}, \quad (15)$$

where $\mathbf{A}, \mathbf{B}, \mathbf{C}, \mathbf{D} \in \mathbb{C}^{J \times 1}$. Thus we have

$$[\hat{\mathbf{h}}_1 \quad \cdots \quad \hat{\mathbf{h}}_{12}] = \begin{bmatrix} \mathcal{J} \otimes \mathbf{A} & \mathcal{J} \otimes \mathbf{B} \\ \mathcal{J} \otimes \mathbf{C} & \mathcal{J} \otimes \mathbf{D} \end{bmatrix}, \quad (16)$$

where \mathcal{J} is a all-ones matrix with the size of $1 \times L$. Therefore, the virtual codebook for the k' -th VN is

$$\hat{\mathbf{C}}_{k'} = \text{diag}(\hat{\mathbf{h}}_{k'}) \begin{bmatrix} \mathbf{C}_g \\ \mathbf{C}_g \end{bmatrix}, \quad (17)$$

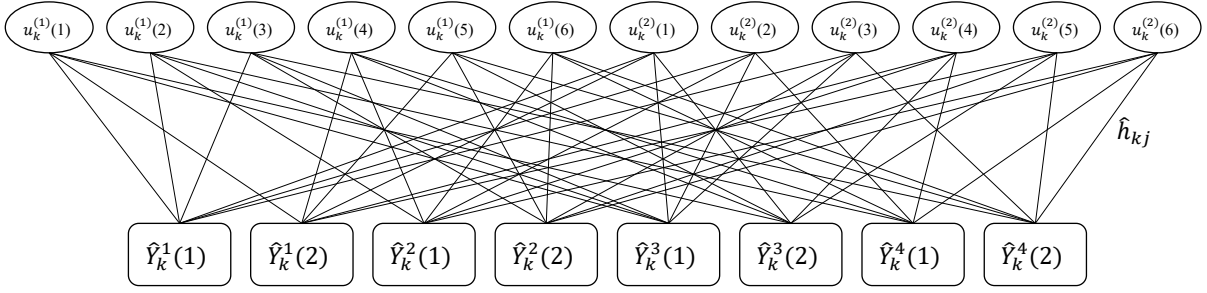


Fig. 5. Factor graph for the k -th user of the joint MPA when $J = 4$, $L = 6$ and $N_t = 2$.

where

$$g = \begin{cases} k', & k' \leq 6 \\ k' - 6, & 6 < k' \leq 12 \end{cases}. \quad (18)$$

With the virtual codebook, we can apply traditional Log-MPA to decode all desired signals.

IV. ERROR RATE ANALYSIS

This section gives the error rate analysis for the proposed CIAMA scheme. Suppose the transmitting power at the BS is equally allocated for users and denote E_b as power allocated for one bit, thus we have

$$\mathbb{E} \left\{ \mathbf{x}_k^j \right\} = \frac{6 \times 6 \times 2E_b}{6 \times 4 \times 2} = \frac{3E_b}{2}. \quad (19)$$

Note that there is a '2' in the denominator of (19), because each symbol is transmitted twice as required by the BIA encoder. For analysis, we denote $\mathbf{x}_k^j = \frac{3E_b}{2} \hat{\mathbf{x}}_k^j$, where $\hat{\mathbf{x}}_k^j$ is normalized transmitting symbol for user- k at the j -th tone. Further we have $\mathbf{X}_k = \frac{3E_b}{2} \mathbf{X}_k^*$, where $\mathbf{X}_k^* = [\hat{\mathbf{x}}_k^1 \ \hat{\mathbf{x}}_k^2 \ \hat{\mathbf{x}}_k^3 \ \hat{\mathbf{x}}_k^4]$.

According to the received signal, the estimated symbols vector $\hat{\mathbf{X}}_k^*$ is determined by

$$\hat{\mathbf{X}}_k^* = \arg \min \left\| \hat{\mathbf{Y}}_k - \sqrt{\frac{3E_b}{2N_0}} \hat{\mathbf{H}}_k \mathbf{X}_k^* \right\|_F^2. \quad (20)$$

The conditional pairwise error probability (PEP) defined as the probability of $\mathbf{X}_k^* \rightarrow \hat{\mathbf{X}}_k^*$ for a fixed channel coefficients can be expressed as

$$\begin{aligned} & Pr \left(\mathbf{X}_k^* \rightarrow \hat{\mathbf{X}}_k^* | \hat{\mathbf{H}}_k \right) \\ &= Q \left(\sqrt{\frac{3E_b}{4N_0}} \left\| \hat{\mathbf{H}}_k (\mathbf{X}_k^* - \hat{\mathbf{X}}_k^*) \right\|_F \right), \end{aligned} \quad (21)$$

where $Q(x) = \frac{1}{\sqrt{2\pi}} \int_x^\infty e^{-\frac{t^2}{2}} dt$. To evaluate (21), we use an upper bound for the Q-function as in [33], thus we have

$$\begin{aligned} & Pr \left(\mathbf{X}_k^* \rightarrow \hat{\mathbf{X}}_k^* | \hat{\mathbf{H}}_k \right) \\ & \leq \sum_{n=1}^N a_n \exp \left(-c_n \frac{3E_b}{4N_0} \left\| \hat{\mathbf{H}}_k (\mathbf{X}_k^* - \hat{\mathbf{X}}_k^*) \right\|_F^2 \right), \end{aligned} \quad (22)$$

where N, a_n, c_n are constants. Note that the upper bound tends to the exact value as N increases.

Since the fact that

$$\begin{aligned} & \left\| \hat{\mathbf{H}}_k (\mathbf{X}_k^* - \hat{\mathbf{X}}_k^*) \right\|_F^2 \\ &= Tr \left(\hat{\mathbf{H}}_k (\mathbf{X}_k^* - \hat{\mathbf{X}}_k^*) (\mathbf{X}_k^* - \hat{\mathbf{X}}_k^*)^H \hat{\mathbf{H}}_k^H \right) \\ &= \sum_{l=1}^8 h_k^l (\mathbf{X}_k^* - \hat{\mathbf{X}}_k^*) (\mathbf{X}_k^* - \hat{\mathbf{X}}_k^*)^H (h_k^l)^H, \end{aligned} \quad (23)$$

where h_k^l is the l -th row vector of $\hat{\mathbf{H}}_k$ and note that the matrix $(\mathbf{X}_k^* - \hat{\mathbf{X}}_k^*) (\mathbf{X}_k^* - \hat{\mathbf{X}}_k^*)^H$ is Hermitian that can be diagonalized by a unitary transformation, thus we have

$$\begin{aligned} & Pr \left(\mathbf{X}_k^* \rightarrow \hat{\mathbf{X}}_k^* | \hat{\mathbf{H}}_k \right) \\ & \leq \sum_{n=1}^N a_n \exp \left(-c_n \frac{3E_b}{4N_0} \sum_{l=1}^8 h_k^l \mathbf{V}_k \mathbf{\Lambda}_k \mathbf{V}_k^H (h_k^l)^H \right) \\ &= \sum_{n=1}^N a_n \exp \left(-c_n \frac{3E_b}{4N_0} \sum_{l=1}^8 \sum_{i=1}^8 \lambda_k^i |h_k^l \mathbf{v}_k^i|^2 \right), \end{aligned} \quad (24)$$

where $\mathbf{\Lambda}_k = \text{diag}(\lambda_k^1, \lambda_k^2, \dots, \lambda_k^8)$. \mathbf{V}_k is a unitary matrix and $\mathbf{v}_k^i = [v_k^{1,i} \ v_k^{2,i} \ \dots \ v_k^{8,i}]$ is the i -th column of \mathbf{V}_k .

In this section, we consider Rayleigh fading channel, i.e., $\mathbf{h}_k^j \sim \mathcal{CN}(\mathbf{0}, \mathbf{I})$. Denotes $|h_k^l \mathbf{v}_k^i|^2$ as $\beta_k^{l,i}$, thus the probability density function of the random variable $\beta_k^{l,i}$ is given by

$f_{\beta_k^{l,i}}(x) = \frac{1}{4b_k^{l,i}} \exp\left(-\frac{x}{4b_k^{l,i}}\right)$, where $b_k^{l,i} = \sum_{j=2^{\lceil \frac{l}{2} \rceil - 1}}^{2^{\lceil \frac{l}{2} \rceil} - 1} T_l |v_k^{j,i}|^2$, where

$$T_l = \begin{cases} \frac{1}{6}, & l \text{ is odd} \\ 1, & l \text{ is even} \end{cases}. \quad (25)$$

Note that T_l comes from the fact that $\mathbf{H}_k^j = \left[\frac{1}{\sqrt{6}} \mathbf{h}_k^j(1) \ \mathbf{h}_k^j(2) \right]^T$.

Then the average PEP has

$$\begin{aligned} & Pr \left(\mathbf{X}_k^* \rightarrow \hat{\mathbf{X}}_k^* \right) \\ & \leq \sum_{n=1}^N a_n \mathbb{E}_{\hat{\mathbf{H}}_k} \left[\exp \left(-c_n \frac{3E_b}{4N_0} \sum_{l=1}^8 \sum_{i=1}^8 \lambda_k^i |h_k^l \mathbf{v}_k^i|^2 \right) \right] \\ &= \sum_{n=1}^N a_n \prod_{l=1}^8 \prod_{i=1}^8 \frac{1}{1 + c_n \frac{3E_b}{4N_0} \lambda_k^i b_k^{l,i}}. \end{aligned} \quad (26)$$

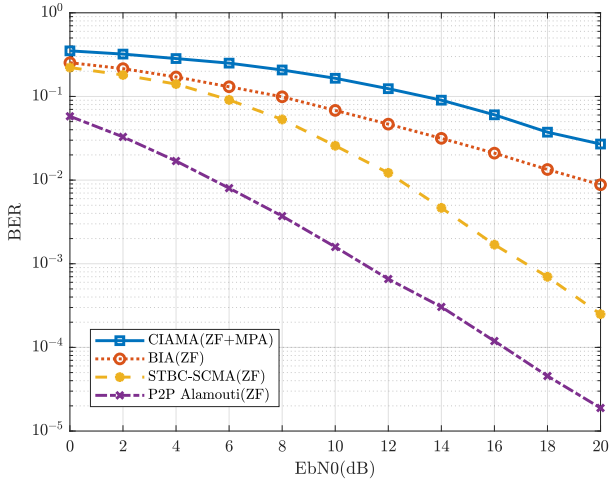


Fig. 6. BER Comparison (Zero-forcing+MPA)

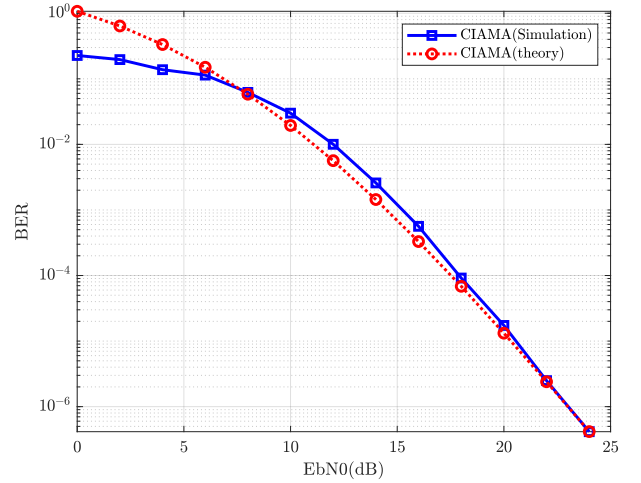


Fig. 8. BER comparison (Simulation. vs Theoretical)

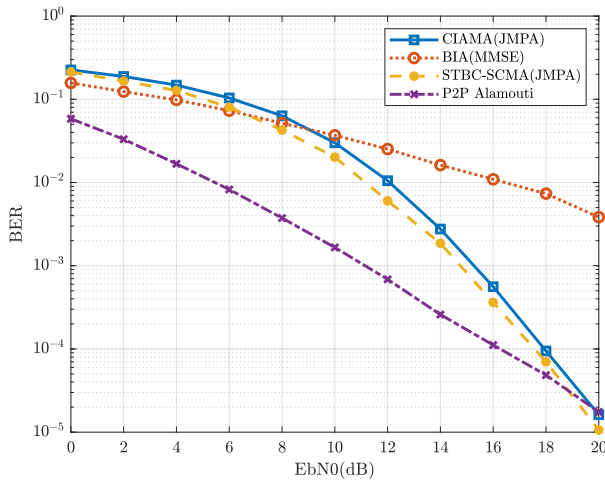


Fig. 7. BER Comparison (Joint MPA)

Hence, the universal bound of bit error rate (BER) should be a weighted version of the PEP

$$\mathbf{BER} = \frac{1}{6} \frac{1}{2^{L \times N_t}} \sum_{i=1}^{2^{L \times N_t}} \sum_{j=1, j \neq i}^{2^{L \times N_t}} Pr(\mathbf{X}_k^i \rightarrow \mathbf{X}_k^j). \quad (27)$$

Denote r as the rank of $(\mathbf{X}_k^i - \mathbf{X}_k^j)$, the minimum r will provide the highest contribution to $Pr(\mathbf{X}_k^i \rightarrow \mathbf{X}_k^j)$, thus the diversity order is obtained by considering the virtue factor graph in Fig. 5 as

$$div = \min r = 4. \quad (28)$$

Note the diversity order in CIAMA is the same as that of STBC-SCMA [32].

V. SIMULATION

In this section, the performance of the proposed CIAMA is compared with traditional BIA and STBC-based SCMA. Also, we consider a Alamouti scheme in a point-to-point 2×1 MISO system as a benchmark in our simulation. Without loss

of generality, we suppose all users have the same distance to the BS.

In Fig. 6, both CIAMA and STBC-SCMA utilize the two-stage ZF+MPA decoder. The BIA and the P2P Alamouti schemes use ZF decoder. We note that the STBC-SCMA has better performance than the BIA, because the SCMA can provide diversity over different tones. Although the ZF+MPA decoder has a lower complexity, the CIAMA experience higher BERs than BIA. That is because the decoder doesn't consider the noise properly and the MPA part does not introduces channel state information. Also, the diversity order of CIAMA is the same as that of BIA, because the MPA in the two stage decoder provides no diversity gain. STBC-SCMA provides a higher diversity gain than CIAMA and BIA, since STBC provides full diversity over multi antennas.

In Fig. 7, both CIAMA and STBC-SCMA utilize a joint MPA decoder and the BIA scheme using a MMSE decoder. From the figure, we can find that the joint MPA can make full use of the benefits due to diversity. Note that STBC can provide spatial diversity, the BIA with joint MPA can also provide it, which is not applicable with ZF or MMSE. Also note that, the decoding complexity of the CIAMA with joint MPA is the same as STBC-SCMA with joint-MPA, but the CIAMA can provide more data flows, e.g., extra multiplexing gain.

Fig. 8 presents the validation of the derived upper bound in (26). The approximation parameter sets are selected as $N = 2$, $a_1 = 1/12$, $a_2 = 1/4$, $c_1 = 1/2$, and $c_2 = 2/3$. The proposed closed-form expression is verified to fit the simulation well, thus it provides a practical criterion to assess the performance of the proposed scheme.

VI. CONCLUSION

This paper proposes an effective CIAMA method to combine BIA and SCMA. The combination method reserves both diversity and multiplexing gain from BIA and SCMA, making it applicable to systems with partial or no channel state information at transmitter side. Moreover, unlike existing MIMO-SCMA schemes, our scheme can yield better data

privacy. Two decoders are proposed for this scheme: a two-stage decoder and a joint message passing algorithm (MPA) decoder. The two-stage decoder has a lower computational complexity, while the joint MPA decoder provides better diversity performance, which allow the proposed method to be implemented under different practical scenarios.

REFERENCES

- [1] M. Shafi et al., "5G: A tutorial overview of standards, trials, challenges, deployment, and practice," *IEEE J. Sel. Areas Commun.*, vol. 35, no. 6, pp. 1201-1221, 2017.
- [2] E. Hossain, M. Rasti, H. Tabassum, and A. Abdelnasser, "Evolution toward 5G multi-tier cellular wireless networks: An interference management perspective," *IEEE Wireless Commun.*, vol. 21, no. 3, pp. 118-127, 2014.
- [3] X. Ge, S. Tu, G. Mao, C.-X. Wang, and T. Han, "5G ultra-dense cellular networks," *IEEE Wireless Commun.*, vol. 23, no. 1, pp. 72-79, 2016.
- [4] X. You et al., "Towards 6G wireless communication networks: vision, enabling technologies, and new paradigm shifts," *Sci. China Inf. Sci.*, vol. 64, no. 110301, 2021.
- [5] N. Himayat, S. Talwar, A. Rao, and R. Soni, "Interference management for 4G cellular standards [WIMAX/LTE UPDATE]," *IEEE Commun. Mag.*, vol. 48, no. 8, pp. 86-92, 2010.
- [6] Z. Ding, X. Lei, G. K. Karagiannidis, R. Schober, J. Yuan, and V. K. Bhargava, "A Survey on Non-Orthogonal Multiple Access for 5G Networks: Research Challenges and Future Trends," *IEEE J. Sel. Areas Commun.*, vol. 35, no. 10, pp. 2181-2195, 2017.
- [7] V. R. Cadambe and S. A. Jafar, "Interference alignment and degrees of freedom of the K -user interference channel," *IEEE Trans. Inf. Theory*, vol. 54, no. 8, pp. 3425-3441, 2008.
- [8] Z. Ding et al., "Application of non-orthogonal multiple access in LTE and 5G networks," *IEEE Commun. Mag.*, vol. 55, no. 2, pp. 185-191, 2017.
- [9] M. A. Maddah-Ali, A. S. Motahari, and A. K. Khandani, "Communication Over MIMO X Channels: Interference Alignment, Decomposition, and Performance Analysis," *IEEE Trans. Inf. Theory*, vol. 54, no. 8, pp. 3457-3470, 2008.
- [10] N. Zhao, F. R. Yu, M. Jin, Q. Yan and V. C. M. Leung, "Interference Alignment and Its Applications: A Survey, Research Issues, and Challenges," *IEEE Commun. Surv. Tutor.*, vol.18, no.3, pp.1779-1803, 2016.
- [11] N. Zhao, F. R. Yu, H. Sun, and M. Li, "Adaptive power allocation schemes for spectrum sharing in interference-alignment-based cognitive radio networks," *IEEE Trans. Veh. Technol.*, vol. 65, no. 5, pp. 3700-3714, 2015.
- [12] C. Suh and D. Tse, "Interference Alignment for Cellular Networks," *46th Annual Allerton Conference on Communication, Control, and Computing.*, pp. 1037-1044, 2008.
- [13] W. Shin, W. Noh, K. Jang, and H.-H. Choi, "Hierarchical interference alignment for downlink heterogeneous networks," *IEEE Trans. Wireless Commun.*, vol. 11, no. 12, pp. 4549-4559, 2012.
- [14] H. E. Elkotby, K. M. Elsayed, and M. H. Ismail, "Exploiting interference alignment for sum rate enhancement in D2D-enabled cellular networks," *IEEE Wireless Communications and Networking Conference (WCNC).*, pp. 1624-1629, 2012.
- [15] Q. F. Zhou, A. Huang, M. Peng, F. Qu and L. Fan, "On the Mode Switching of Reconfigurable-Antenna-Based Blind Interference Alignment," *IEEE Trans. Veh. Technol.*, vol. 66, no. 8, pp. 6958-6968, 2017.
- [16] L. Dai, B. Wang, Y. Yuan, S. Han, I. C. and Z. Wang, "Non-orthogonal multiple access for 5G: solutions, challenges, opportunities, and future research trends," *IEEE Commun. Mag.*, vol. 53, no. 9, pp. 74-81, 2015.
- [17] Z. Ding and H. V. Poor, "Design of massive-MIMO-NOMA with limited feedback," *IEEE Signal Process Lett.*, vol. 23, no. 5, pp. 629-633, 2016.
- [18] D. Zhang, Z. Zhou, C. Xu, Y. Zhang, J. Rodriguez, and T. Sato, "Capacity analysis of NOMA with mmWave massive MIMO systems," *IEEE J. Sel. Areas Commun.*, vol. 35, no. 7, pp. 1606-1618, 2017.
- [19] S. M. Razavi and T. Ratnarajah, "Performance analysis of interference alignment under CSI mismatch," *IEEE Trans. Veh. Technol.*, vol. 63, no. 9, pp. 4740-4748, 2014.
- [20] T. Gou, C. Wang and S. A. Jafar, "Aiming Perfectly in the Dark-Blind Interference Alignment Through Staggered Antenna Switching," *IEEE Trans. Signal Process.*, vol. 59, no. 6, pp. 2734-2744, 2011.
- [21] Q. F. Zhou, Q. T. Zhang and F. C. M. Lau, "Diophantine Approach to Blind Interference Alignment of Homogeneous K-User 2x1 MISO Broadcast Channels," *IEEE J. Sel. Areas Commun.*, vol. 31, no. 10, pp. 2141-2153, 2013.
- [22] J. Wu, X. Liu, C. Qu, C. -T. Cheng and Q. Zhou, "Balanced-Switching-Oriented Blind Interference-Alignment Scheme for 2-User MISO Interference Channel," *IEEE Commun. Lett.*, vol. 24, no. 10, pp. 2324-2328, 2020.
- [23] V. M. U and P. Selvaprabhu, "Blind interference alignment: A comprehensive survey," *Int J Commun Syst.*, vol.35, no.8, p.e5116, 2022.
- [24] S. M. R. Islam, N. Avazov, O. A. Dobre, and K. Kwak, "Power-Domain Non-Orthogonal Multiple Access (NOMA) in 5G Systems: Potentials and Challenges," *IEEE Commun. Surv. Tutor.*, vol. 19, no. 2, pp. 721-742, 2017.
- [25] Z. Q. Al-Abbasi, D. K. C. So, and J. Tang, "Resource allocation for MU-MIMO non-orthogonal multiple access (NOMA) system with interference alignment," *IEEE International Conference on Communications (ICC)*, 2017.
- [26] A. Nasser, O. Muta, M. Elsabrouty, and H. Gacanin, "Interference Mitigation and Power Allocation Scheme for Downlink MIMO-NOMA HetNet," *IEEE Trans. Veh. Technol.*, vol. 68, no. 7, pp. 6805-6816, 2019.
- [27] M. Morales-Céspedes, O. A. Dobre and A. García-Armada, "Semi-Blind Interference Aligned NOMA for Downlink MU-MISO Systems," *IEEE Trans. Commun.*, vol.68, no.3, pp.1852-1865, 2020.
- [28] H. Nikopour and H. Baligh, "Sparse code multiple access," *IEEE 24th Annual International Symposium on Personal, Indoor, and Mobile Radio Communications (PIMRC).*, pp.332-336, 2013.
- [29] M. Taherzadeh, H. Nikopour, A. Bayesteh and H. Baligh, "SCMA Codebook Design," *IEEE 80th Vehicular Technology Conference (VTC2014-Fall).*, pp. 1-5, 2014.
- [30] Y. -M. Chen and J. -W. Chen. "On the design of near-optimal sparse code multiple access codebooks," *IEEE Trans. Commun.*, vol.68, no.5, pp.2950-2962, 2020.
- [31] Y. -M. Chen, Y. -C. Hsu, M. -C. Wu, R. Singh and Y. -C. Chang, "On Near-Optimal Codebook and Receiver Designs for MIMO-SCMA Schemes," *IEEE Trans. Wireless Commun.*, vol.21, no.12, pp.10724-10738, 2022.
- [32] Z. Pan, W. Liu, J. Lei, J. Luo, L. Wen and C. Tang, "Multi-Dimensional Space-Time Block Coding Aided Downlink MIMO-SCMA," *IEEE Trans. Veh. Technol.*, vol.68, no.7, pp.6657-6669, 2019.
- [33] M. Chiani, D. Dardari and M. K. Simon, "New exponential bounds and approximations for the computation of error probability in fading channels," *IEEE Trans. Wireless Commun.*, vol.2, no.4, pp.840-845, 2003.